CLIMA 2016 - proceedings of the 12th REHVA World Congress

volume 3

Heiselberg, Per Kvols

Publication date:
2016

Document Version
Publisher's PDF, also known as Version of record

Double Skin Façades Integrating Photovoltaic Panels: A Comparative Analysis of the Thermal and Electrical Performance

Z. Ioannidis[1], A. Buonomano[2], A.K. Athienitis[1], T. Stathopoulos[1]

[1]*Centre for Zero Energy Building Studies, Department of Building, Civil and Environmental Engineering, Concordia University, 1455 de Maisonneuve Blvd. W., Montreal, H3G 1M8 QC, Canada*

[2]*DII, University of Naples Federico II, P.le Tecchio, 80, 80125 Naples, Italy*

[1]z_ioann@encs.concordia.ca

Abstract

A numerical model is developed for simulating a single or multi–story Double Skin Façade integrating Photovoltaics (DSF-P). The proposed model enables the prediction of the thermal and electrical performance of the DSF-P system. The DSF-P can co-generate solar electricity and heat. The buoyancy-driven air flow inside the cavity may be assisted by a fan to cool down the photovoltaics while providing natural or hybrid ventilation to adjacent zones. Automated roller shades are also implemented in the model, which help regulate heating and cooling loads but also control the daylight levels in the indoor space. A comparative analysis for two different climate zones, Montreal (Canada) and Naples (Italy), is performed with the purpose to apply the proposed methodology for the optimization of the DSF-P system in different climate regions. The simulations show that a DSF-P system integrating photovoltaics can supply approximately 0.20kWh/m2/day of solar electricity to the adjacent office space covering the daily thermal energy demand of the office (cooling and heating). In addition, during the heating period for a three-story DSF-P, the temperature difference between the inlet and the outlet of the cavity can reach up to 18°C giving the opportunity for natural or hybrid ventilation to the building.

Keywords: Double Skin Façade, BIPV, BIPV/T, Photovoltaics, multi-story, energy consumption.

1. Introduction

Office buildings may have high energy consumption but they also have much potential for energy savings. The possibility of using the solar radiation to satisfy all the energy needs of the building has led to the design and research of net-zero energy buildings (NZEB) [1]. One of the key new features sometimes employed in high-rise buildings is double skin façades (DSF). A DSF normally consists of an external and an internal skin separated by a cavity that is used as an air channel (Figure 1) [2]. This cavity is a buffer zone and it is created between the exterior skin and the insulated interior skin, which alone could be the façade of a newly built or a renovated building. In this way, DSF can create a microclimate around the building adding climate resilience to it and assisting it to adapt to ambient temperature fluctuations. Temperature differences inside the cavity can be controlled in order to recover heat from it or facilitate natural ventilation, while the exterior skin can be used to integrate photovoltaics.

Nomenclature

A	heat exchange surface area (m^2)
C	thermal capacitance (J/K)
c_p	specific heat capacity (kJ/kgK)
DSF-P	Double Skin Façade integrating Photovoltaics
E	total emissive power (W/m^2)
f	surface view factor (-)
H	total DSF height (m)
H_1	opaque PV height (m)
H_2	exterior glazing height (m)
H_3	ST-PV panel height (m)
I	solar radiation flux (W/m^2)
J	radiosity (W/m^2)
L	room length (m)
$\dot{m}$	mass flow rate (kg/s)
N	node of the thermal network
$\dot{Q}$	thermal load (W)
PV	photovoltaic
R	thermal resistance (K/W)
SP	semi transparent
T	temperature (K)
t	time (s)
V	velocity (m/s)
W	room width (m)
Z	building space

Greeks letters	
α	absorption factor (-)
ε	emissivity (-)
η	photovoltaic efficiency (-)
σ	Stefan-Boltzmann constant ($5.67\ 10^{-8}\ W/m^2K^4$)
Superscript/Subscripts	
air	air of the channel
ch	channel
db	dry bulb air
el	electricity
ext	external
f	façade
fl	floor
in	indoor air
int	internal
n	node of the thermal network
PV	photovoltaic
rad	radiation
sky	sky vault
wg	referred to water vapour gain
wi	interior wall section
wl	wall
wo	exterior wall section
z	building space

DSF can contribute to the reduction of the energy consumption of buildings by behaving as a buffer zone that can interact with the adjacent zones and the environment. Also DSF has significant potential for daylight control and energy savings through the use of louvers or blinds [3]–[5]. In addition, DSF can improve acoustic comfort, protect the building from wind or rain penetration while it reduces the heating or cooling loads of the building [6]–[8]. In particular, to avoid rain penetration, one type of DSF, also named rainscreen wall, applies pressure equalization for which airflow and pressures inside the cavity are important [9]. DSF also provide the opportunity to use operable windows and at the same time extend the usable indoor space area near the window. Furthermore, DSF can be an extremely suitable source for natural or hybrid ventilation for the building [6].

The integration of photovoltaics on the exterior skin along with the implementation of controlled shading devices in the middle of the cavity of a DSF, gives the opportunity to design an energy positive DSF façade. This can be achieved by combining three different features of the DSF:

- Electricity generation from the integrated opaque or semi-transparent photovoltaics;
- Solar heat gains and daylight control through the use of shading devices located between the exterior and interior skin of a DSF;
- Extraction of heat from the photovoltaics and the shading device which is recovered by the air flowing inside the cavity.

This technology has been widely reviewed in the past, concluding that the main research was focused on the ventilation of the DSF, whereas daylighting [7], integration of semitransparent photovoltaics and wind effects have not been studied yet. Clearly it is very difficult to achieve natural ventilation all year round and that a hybrid system should be developed [10]. Since there was no standard way on reporting results among the researchers, De Gracia et al [11] suggested that further research is required to compare all models with the same experimental test, although many studies have focused only on the DSF cavity and not at its interior adjacent zones [10].

The heat transfer phenomena in an airflow window with BIPV/T were extensively studied [12], while the optimization of the performance of DSF with integrated opaque photovoltaics [13] and semi-transparent photovoltaics, [14], [15] were only recently analyzed. However very few studies have focused on the description of the behavior of integrated photovoltaics on double skin façades.

2. Modeling

In this paper a numerical model for the assessment of the energy performance of a multi-story Double Skin Façade (DSF) has been implemented in MatLab (Mathworks). The model has the ability to simulate the opaque or semi-transparent photovoltaics integrated on the exterior layer of the double skin façade as well as any shading devices inside the cavity including the shades that they provide to the building (Figure 1). It is also capable to assess the active and passive effects of the generic DSF-P on the thermal and visual comfort and energy consumptions of the building in which the system is integrated. The model also allows the user to perform a parametric analysis by changing the design, and geometric parameters and the optical, thermal and flow properties of the DSF. The set of parameters to be varied are reported in Table 1.

Thus, the whole façade, and, similarly, the wall of a multi-story building are designed as multiple strips made of semi-transparent (ST), transparent, and opaque elements. Roller shades/blinds are located in the middle of the cavity in order to control the daylighting levels within the indoor space. Air can flow on both sides of the shading devices placed within the cavity (Figure 1). The simulation model of the DSF-P takes into account all of the heat transfer processes, utilizes an accurate nodal approach, and uses fast numerical solving processes. A set of explicit finite difference equations is obtained for each node of the adopted thermal network, showing the conductive, radiative and convective heat transfers in the DSF-P system modelled (Figure 2).

In order to capture the gradient of the air temperature along the cavity, each element of the multi-story DSF-P (i.e. the façade, the two air channels, and the wall) is subdivided, along the vertical direction, in N equal control volumes (i.e. N is suitably selected to

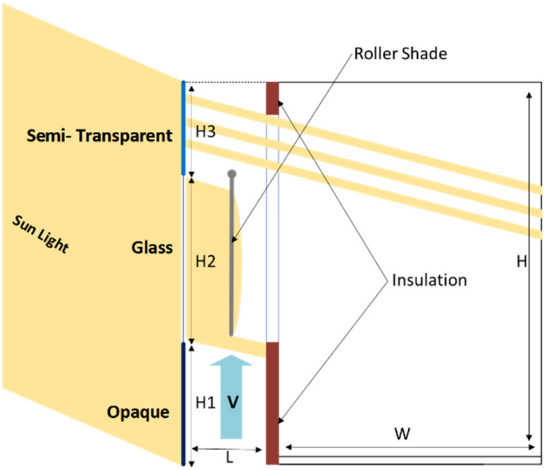

Figure 1 *Sketch of the double façade section (one floor)*

Table 1 Input parameters of the numerical model

Design parameters	Number of floors	**Optical properties**	STPV transmittance
	Position of PV		Roller shade transmittance
	Position of roller blind		Glazing transmittance
	Interior skin design		PV efficiencies
Geometric parameters	H1/H	**Thermal properties**	Roller emissivity
	H2/H		SHCG
	H3/H		Insulation of the room
	L/H	**Flow properties**	Reynolds number
	W/H		Velocity

enhance the accuracy of the simulation results), whose temperatures are calculated through the energy balance method. The multi-story building adjacent to the DSF-P is subdivided in *Z* different perimeter thermal zones as well.

Therefore, in each time step *t*, for each *z*-th perimeter zone and for each *n*-th section/node of the façade, the corresponding energy balance equation is calculated as:

$$\sum_{i=n-1}^{n+1} \frac{T_{f,i}-T_{f,n}}{R_{f,i}} + \frac{T_{db}-T_{f,n}}{R_{ext,n}} + \frac{T_{air,n}-T_{f,n}}{R_{ch,n}} + \dot{Q}_{f,n} + \dot{Q}_{rad,n} = 0 \qquad (1)$$

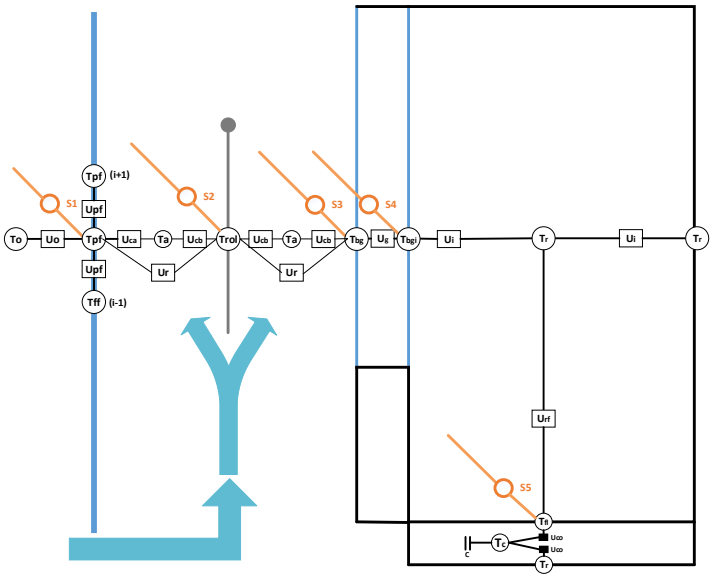

Figure 2 *Sketch of the modelled RC thermal network*

The radiative heat transfer problem within the channel is solved by assessing the view factors and the radiosities of all sections constituting the cavity included between the façade and the facing surfaces, i.e. roller shades and/or wall.

The following equations include the diffuse solar radiation and the net (transmitted and/or absorbed) beam solar radiation, suitably calculated by taking into account the cast shadows due to the façade surfaces and the roller blinds. In addition, the thermal resistance of the roller blind is considered negligible while it is assumed that no air passes through the shade [17].

$$\dot{Q}_{f,n} = \left[\alpha_{f,n} \cdot I_{f,n} + \varepsilon_n \cdot \sigma \cdot f \cdot (T_{sky}^4 - T_{f,n}^4)\right] \cdot A_n$$
$$\dot{Q}_{rad,n} = A_n \cdot \sum_{i=1}^{N} \frac{\varepsilon_i}{1-\varepsilon_i} \cdot (E_{n,i} - J_i) \tag{2}$$

$$\frac{T_{air,n} - T_{wo,n}}{R_{ch,n}} + \frac{T_{wi,n} - T_{wo,n}}{R_{wl,n}} + \dot{Q}_{wo,n} + \dot{Q}_{rad,n} = 0$$
$$\frac{T_{wo,n} - T_{wi,n}}{R_{wl,n}} + \frac{T_{in,k} - T_{wi,n}}{R_{int,n}} + \dot{Q}_{wi,n} = 0 \tag{3}$$

The buoyancy-driven air flow in the cavity is assumed to be quasi-steady and for each of the N control volumes in which each air channel is discretized, an energy balance is written. It must be noted that, due to the adopted formulation, the air temperature of the channels inside the double façade describes the radiation exchange, convection and mass transfer, including the identification of the heat transfer coefficients. It is worth noting that, as reported in previous studies, the temperature profile in a ventilated cavity is exponential [13]. Thus, with the aim to avoid the use of an air temperature profile, the change of energy of each control volume is assumed equal to the energy transferred to the air by convection. This leads, after solving a first order differential equation of air temperature [13], to an expression that easily provides an exponential profile.

$$T_{air,n} = \exp\left(-\frac{{R_{ch,n}}^{-1} + {R_{ext,n}}^{-1}}{\dot{m}_{air} \cdot c_{p,air}}\right) \cdot T_{air,n-1} + \left[1 - \exp\left(-\frac{{R_{ch,n}}^{-1} + {R_{ext,n}}^{-1}}{\dot{m}_{air} \cdot c_{p,air}}\right)\right] \times \ldots \times \left(\frac{{R_{ch,n}}^{-1} \cdot T_{f,n} + {R_{ext,n}}^{-1} \cdot T_{wo,n}}{{R_{ch,n}}^{-1} + {R_{ext,n}}^{-1}}\right) \quad (4)$$

Note that, depending on the channel, different boundary conditions are taken into account and that, no air leakage is assumed in the DSF-P cavity. It is also assumed that uniform solar radiation is incident on clean exterior surfaces and PV modules are operating at their maximum power point condition.

For each z-th indoor space adjacent to the DSF-P system, its indoor air is assumed as uniform and perfectly mixed. Therefore, a single lumped indoor air temperature node is taken into account. In order to assess the transient effects induced by the thermal mass, the floor thermal mass is lumped in a single capacitive node, whereas the thermal effect of interior walls are disregarded (i.e. also assuming the same temperature in the core zones of the whole building). This entails that for each z-th zone, the differential equations describing the energy rate of change of each temperature node of the air and floor is calculated as:

$$T_{fl,z}^{t} = T_{fl,z}^{t-1} + \frac{\Delta t}{C_{fl,z}} \cdot \left(\dot{Q}_{fl,z} + \sum_{k=1}^{N} \frac{T_{wi,k} - T_{fl,z}^{t-1}}{\bar{R}_{rad,k}} + \frac{T_{in,z} - T_{fl,z}^{t-1}}{R_{fl,int}}\right) \quad (5)$$

$$T_{in,z}^{t} = T_{in,z}^{t-1} + \frac{\Delta t}{C_{in,z}} \cdot \left(\dot{Q}_{in,z} + \sum_{k=1}^{N} \frac{T_{wi,k} - T_{in,z}^{t-1}}{\bar{R}_{int,k}} + \frac{T_{fl,z} - T_{in,z}^{t-1}}{R_{fl,int}}\right) \quad (6)$$

$\bar{R}_{rad}$ and $\bar{R}_{int}$ is the radiative thermal resistance between the internal wall surfaces and the floor and between the internal wall surfaces and the indoor respectively. By following this approach, thermal power is added to or subtracted from $\dot{Q}_{in,z}$ with the aim to maintain the indoor air temperature at the desired set points.

3. Simulation

The simulations were carried out for a winter and a summer month (January and August respectively). The indoor office conditions were following a normal week-day schedule from 8.00 to 18:00 and the temperature was let to fluctuate between 21°C and

24°C. The simulation were carried out with one hour time step, compatible with Typical Meteorological Year data files (TMY), used as a source for the ambient weather conditions and the solar radiation. The considered climate zones refer to: i) Montreal (Canada), featuring a semi-continental climate, with a very cold snowy winter and a warm and hot summer; ii) Naples (Italy), characterized by a typical Mediterranean climate with hot and dry summer and a mild winter. A reference office described by Reinhart et al. [18] was taken into account; with dimensions 2.8m height, 3.6m width and 8.2m length. The bottom spandrel is 1.0m high, the window is 1.5m high and the upper spandrel is 0.3m high giving a 55% window-to-wall ratio. The cavity width is set to be 0.5m, the roller is placed at the middle of the DSF-P cavity (0.25m from both ends) and the transmittance of the STPV is set to be 30%. A three-story DSF-P model was simulated for two different set-ups. One with the roller blind completely shading the interior space (later labelled as roller down), and one with the roller blind rolled up (later labelled as roller up). Also the velocity of the air inside the DSF-P cavity was set to 0.2 m/s.

4. Results

Air temperature difference (ΔT) between the inlet and the outlet of the DSF cavity is simulated for all different cases presented above. The maximum ΔT is illustrated on Table 2. A typical roller blind may result into a 33% higher temperature difference between the inlet and the outlet of a three-floor high DSF due to the energy trapped inside the cavity by the added blinds (18.20°C with blind and 13.73°C without). In the case of the roller down scenario, as the solar radiation is absorbed by the roller blind devices, the temperature inside the cavity increases. On the contrary, in the roller up scenario, most of the solar radiation enters the adjacent indoor spaces through the large glazing surface. In addition, in the roller down scenario, for both the investigated weather locations, the maximum ΔT occurs if solar radiation and ambient temperature are simultaneously hight. In the roller up scenario, a lower influence of the solar radiation on the ΔT, with respect to the ambient temperature is noticed. In fact, while in January, the maximum ΔT is observed in Naples (i.e. higher solar radiation), in August, by comparing the results obtained in Montreal and Naples, a negligible difference is detected due to comparable weather conditions (Table 2). This temperature difference is very important because the cavity may work as a buffer zone during the cold months of the year and the preheated air may be introduced to the HVAC system. From Table 2 it is clear that the first floor contributes the most on the ΔT between the inlet and the outlet of the DSF-P and that the temperature difference between the inlet and the outlet of every floor is decreasing linearly for all cases examined. This is something that is expected because the temperature difference between the air and the surfaces of the DSF-P is greater at the beginning of the channel. It should also be noted that the temperature differences between the inlet and the outlet of the DSF that appear at the solar noor of every day are of equivilent magnitute. The ambient temperature of the air at which the maximum ΔT occurs for roller down position is 0.4°C and 28.35°C for Montreal and 14.45°C and 26.85°C for Naples for January and August respectively.

Table 2 Maximum temperature difference between the inlet and the outlet for all cases examined

Temperature difference (°C)						
	Floors	Montreal			Naples	
		Roller down	Roller up		Roller down	Roller up
January	Tout	0.40		Tout	14.45	
	1st	6.14	4.80		6.72	5.10
	2nd	5.57	4.35		6.05	4.56
	3rd	5.05	3.92		5.43	4.07
	DSF	16.76	13.07		18.20	13.73
August	Tout	28.35		Tout	26.85	
	1st	4.55	4.00		4.58	4.04
	2nd	4.05	3.58		4.08	3.56
	3rd	3.61	3.12		3.64	3.18
	DSF	12.21	10.70		12.30	10.78

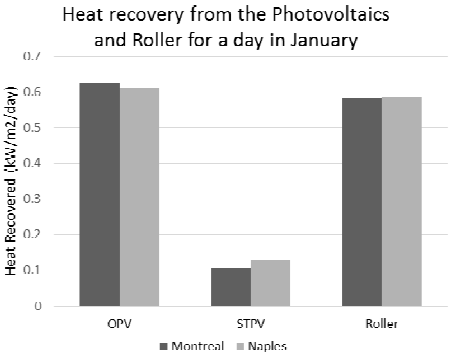

Figure 3 *Heat recovery from Opaque PV (OPV), Semi-transparent PV (STPV) and Roller - average day in January.*

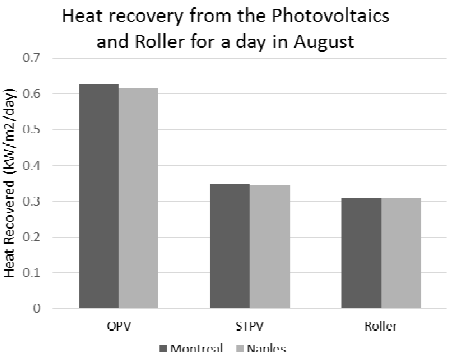

Figure 4 *Heat recovery from Opaque PV (OPV), Semi-transparent PV (STPV) and Roller - average day in August.*

Figures 3 and 4 present the heat recovered from the DSF-P system. The results are reported for January 1st and August 1st. These two days can be presented as typical January and August days because they do not stand out from the average weather conditions for these two months. A comparison between Montreal and Naples is also held in these two graphs showing that the two cities follow the same pattern for the two months. Also the heat recovered from the Opaque Photovoltaic (OPV) per square meter for a day is the same for the two different months examined. The difference is located on the Semi-transparent PV and the roller where we have a difference of 70% and 50% respectively on the heat recovered per square meter per day between the two different months.

The other parameter that is of equal importance to the temperatures of the cavity and the heat recovered from the PV and roller is the energy consumption and generation of the system. For a typical schedule (8.00 to 18:00), the energy required to maintain the indoor air temperature of the adjacent zones at the selected set points (between 21°C and 24°C) is presented in Figure 5 and Figure 6, for January and August respectively. On the same graphs, a comparison between the electrical energy produced by the photovoltaic panels integrated on the DSF-P and the energy consumed to heat or cool the rooms for the three floors is shown. A heat pump with a coefficient of performance equal to 2.5 is assumed to be the source of heating and cooling to the interior zone [19]. For the winter when only heating is needed, the total amount of energy used to heat or cool the room can be produced entirely by the photovoltaics On Figure 5, for Montreal, it is clear that the energy consumption per floor decreases gradually as the number of the floor increases. The opposite is shown on Figure 6. This is something that is expected and it is in accordance with the results shown on Table 2, because the temperature of the DSF-P cavity rises as we go further away from the inlet. This results in lower energy consumption for the higher floors when heating is required for the adjacent zones and higher energy consumption for the upper floors when cooling is needed.

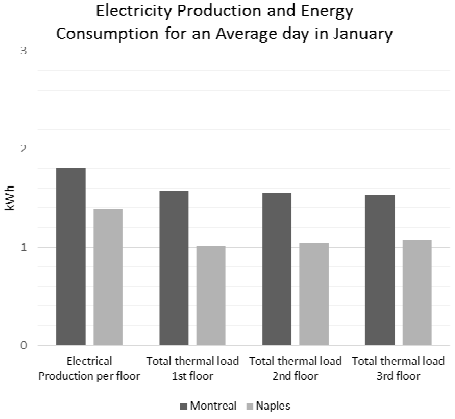

Figure 5 *Energy production from the PV integrated on the façade in comparison to the total energy requirement (for every floor) - average day in January.*

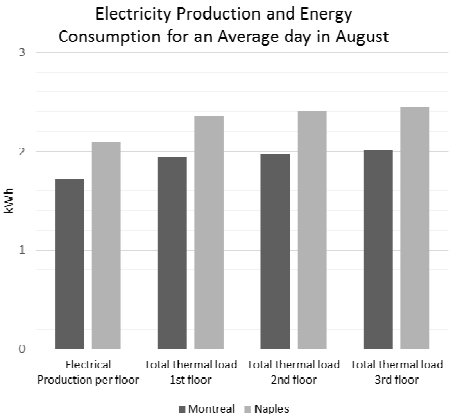

Figure 6 *Energy production from the PV integrated on the façade in comparison to the total energy requirement (for every floor) - average day in August.*

5. Conclusion

In this paper a numerical model of a Double Skin Façade integrated with photovoltaics (DSF-P) is presented. The paper also reports the methodology followed and the equations used in order to simulate the thermal and energy performance of the multi-story DSF-P system. With the aim to show the capability of the numerical model, a set of simulations was carried out for January and August in Montreal and Naples for

different set-up of the roller blind located at the centre of the DSF cavity (e.g. shade, no shade).

It is noted that the existence of a roller blind increases the temperature of the air inside the cavity and the temperature difference between the inlet and the outlet. The simulations show that by means of simulated DSF-P system for a typical office, the integrated photovoltaic panels can provide a big percentage of the energy used to heat or cool the interior adjacent zones by supplying approximately 0.20kWh/m2/day of solar electricity. By introducing the preheated air of the DSF-P to the HVAC system, the PV may be able to cover a large percentage of all the energy needs of the building.

Finally, a simulation model that can assess the performance of a double skin façade integrated with photovoltaics was developed to aid the design of net-zero energy buildings. The simulation model allows parametric and sensitivity analyses and it can be used for pre-feasibility studies at the design phase of new buildings or for retrofit projects.

References

[1] A. Athienitis and W. O'Brien, *Modeling, Design, and Optimization of Net-Zero Energy Buildings*. 2015.

[2] D. Saelens, J. Carmeliet, and H. Hens, "Energy Performance Assessment of Multiple-Skin Facades," *HVAC&R Res.*, vol. 9, no. 2, pp. 167–185, 2003.

[3] E. Gratia and A. De Herde, "The most efficient position of shading devices in a double-skin facade," *Energy Build.*, vol. 39, pp. 364–373, 2007.

[4] H. Manz, "Total solar energy transmittance of glass double fa??ades with free convection," *Energy Build.*, vol. 36, no. 2, pp. 127–136, 2004.

[5] D. Saelens, S. Roels, and H. Hens, "Strategies to improve the energy performance of multiple-skin facades," *Build. Environ.*, vol. 43, pp. 638–650, 2008.

[6] E. Gratia and A. De Herde, "Are energy consumptions decreased with the addition of a double-skin?," *Energy Build.*, vol. 39, pp. 605–619, 2007.

[7] M. a. Shameri, M. a. Alghoul, K. Sopian, M. F. M. Zain, and O. Elayeb, "Perspectives of double skin façade systems in buildings and energy saving," *Renew. Sustain. Energy Rev.*, vol. 15, no. 3, pp. 1468–1475, 2011.

[8] G. Quesada, D. Rousse, Y. Dutil, M. Badache, and S. Hallé, "A comprehensive review of solar facades. Transparent and translucent solar facades," *Renew. Sustain. Energy Rev.*, vol. 16, no. 5, pp. 2643–2651, 2012.

[9] S. Kala, T. Stathopoulos, and K. Suresh Kumar, "Wind loads on rainscreen walls: Boundary-layer wind tunnel experiments," *J. Wind Eng. Ind. Aerodyn.*, vol. 96, no. 6–7, pp. 1058–1073, 2008.

[10] S. Barbosa and K. Ip, "Perspectives of double skin façades for naturally ventilated buildings: A review," *Renew. Sustain. Energy Rev.*, vol. 40, pp. 1019–1029, 2014.

[11] A. De Gracia, A. Castell, L. Navarro, E. Oró, and L. F. Cabeza, "Numerical modelling of ventilated facades: A review," *Renew. Sustain. Energy Rev.*, vol. 22, pp. 539–549, 2013.

[12] L. Liao, a. K. Athienitis, L. Candanedo, K.-W. Park, Y. Poissant, and M. Collins, "Numerical and Experimental Study of Heat Transfer in a BIPV-Thermal System," *J. Sol. Energy Eng.*, vol. 129, no. 4, p. 423, 2007.

[13] R. Charron and A. K. Athienitis, "Optimization of the performance of double-façades with integrated photovoltaic panels and motorized blinds," *Sol. Energy*, vol. 80, pp. 482–491, 2006.

[14] L. Gaillard, C. Ménézo, S. Giroux, H. Pabiou, and R. Le-Berre, "Experimental Study of Thermal Response of PV Modules Integrated into Naturally-ventilated Double Skin Facades," *Energy Procedia*, vol. 48, pp. 1254– 1261, 2014.

[15] L. Gaillard, S. Giroux-Julien, C. Ménézo, and H. Pabiou, "Experimental evaluation of a naturally ventilated PV double-skin building envelope in real operating conditions," *Sol. Energy*, vol. 103, pp. 223–241, 2014.

[16] Matlab, "Matworks," *2016*. [Online]. Available: http://www.mathworks.com/.

[17] N. Safer, M. Woloszyn, and J. J. Roux, "Three-dimensional simulation with a CFD tool of the airflow phenomena in single floor double-skin facade equipped with a venetian blind," *Sol. Energy*, vol. 79, pp. 193–203, 2005.

[18] C. F. Reinhart, J. A. Jakubiec, and D. Ibarra, "DEFINITION OF A REFERENCE OFFICE FOR STANDARDIZED EVALUATIONS OF DYNAMIC FAÇADE AND LIGHTING TECHNOLOGIES 1 Massachusetts Institute of Technology, Cambridge , MA 02139 , USA 2 Harvard University , Graduate School of Design, Cambridge, MA 02138, USA," *13th Conf. Int. Build. Perform. Simul. Assoc.*, pp. 3645–3652, 2013.

[19] ASHRAE, *ASHRAE HANDBOOK HVAC Systems and Equipment*. 2008.